Table S1, related to Figures 1, 4. CFS break-frequency in Aph-treated K562 cells (see attached Excel file)

shRNAs	**Sequence (5'-3')**
sh-RFP	5'-CGTAATGCAGAAGAAGACCAT-3'
sh-mH2A1.2	5'-CTGAACCTTATTCACAGTGAA-3'
sh-SPT16 #1	5'-CCCTGTGATGGAGAAATGATT-3'
sh-SPT16 #2	5'-CCTAGAATACCCTGATGAGAA-3'
sh-SSRP1	5'-GCATGGCAAGACCTTTGACTA-3'
siRNAs	**Sequence (5'-3')**
si-mH2A1.2 #1	5'-GCUUUGAGGUGGAGGCCAUUU-3'
si-mH2A1.2 #2	5'-CUGAACCUUAUUCACAGUGAAUU-3'
si-p53	5'-GAAAUUUGCGUGUGGAGUA-3'
si-ATM	ON-TARGET smart-pool (Dharmacon)
si-control	ON-TARGET smart-pool (Dharmacon)
gRNAs	**Sequence (5'-3')**
5'-ex6a	5'-GAGCATGAGGTGGGAAATAAC-3'
3'-ex6a	5'-GATTGACCTTAAAGATGACCT-3'

Table S2, related to STARS Methods. siRNA/shRNA and gRNA sequences.

Primer Name	Sequence (5'-3')
ChIP-qPCR	
NFS-1-Chr15 F	5'-GGAAGAGGAGGATAACAGCAATAG-3'
NFS-1-Chr15 R	5'-AAATGGACAGGGCGTTTACT-3'
NFS-2-Chr1 F	5'-ATGTTCCCCAAGCAGTGTTC-3'
NFS-2-Chr1 R	5'-CAGAAGGAGCCCAGAGATTTT-3'
FRA1I F	5'-CAAATTGCAGGCAGGCTTATAG-3'
FRA1I R	5'-TGATTGCGCCACTGTACTT-3'
FRA3B F	5'-TGTTGGAATGTTAACTCTATCCCAT-3'
FRA3B R	5'-ATATCTCATCAAGACCGCTGCA-3'
FRA3He F	5'-TGAGGACCGATGGAGATAGAA-3'
FRA3He R	5'-TCTTAGGAGGGTGGGAGAATAA-3'
FRA3O F	5'-CTTGGTCTCACAGCCAGAAA-3'
FRA3O R	5'-GTCACAGTAATCACCCAGGAAG-3'
FRA9I F	5'-TAAAGGACTCCAAAGGCCTAA-3'
FRA9I R	5'-CTGGTCCAGCTGATAGAGAAAC-3'
FRA10A F	5'-CGTGACTTTGTGGCACTTTG-3'
FRA10A R	5'-CTGGGATGGTTGCATTTGTATG-3'
FRA10C F	5'-GGTAACACTACACTGCCCTTT-3'
FRA10C R	5'-CGGCCAGTTCCTGTAACTATAC-3'
FRA11G F	5'-ACTCTCTGTGCCTTCGTTTC-3'
FRA11G R	5'-GGCAACATTCTGAGCACTTATG-3'
FRA15E F	5'-CACTCTCCAGTGCTCACATTAC-3'
FRA15E R	5'-AGTGACAGATCATCAGGCATTAG-3'
FRA16D F	5'-GAGCCTATTGTACCAGCTACTC-3'
FRA16D R	5'-GATCTCAGCCCACTTCAATCT-3'
FRA17E F	5'-GCTAGGAGCCAGAACCTATAAAC-3'
FRA17E R	5'-ACACTTTGAATGGAGTCAGTAT-3'
FRA20E F	5'-GTTTGCTTGAGCTGCCATTAC-3'
FRA20E R	5'-CCAACCTTGATCTTGGACTTCT-3'
RT-PCR	
mH2A1.2 F	5'-GCTTTGAGGTGGAGGCCATAATCA-3'
mH2A1.2 R	5'-ACTCCTTGCCACCTTTCTTCTCCA-3'
p16 F	5'-GAAGGTCCCTCAGACATCCCC-3'
p16 R	5'-CCCTGTAGGACCTTCGGTGAC-3'
p21 F	5'-CAGGGGACAGCAGAGGAAGA-3'
p21 R	5'-TTAGGGCTTCCTCTTGGAGAA-3'
β-actin F	5'-TTCTACAATGAGCTGCGTGTGGCT-3'
β-actin R	5'-TCATCTTCTCGCGGTTGGCCT-3'

Rpl13a F	5’-GAAGTACCAGGCAGTGACAG-3’
Rpl13a R	5’-GGTCTTGAGGACCTCTGTG-3’
GAPDH F	5’-GGAGTCAACGGATTTGGTCG-3’
GAPDH R	5’-GAGGCATTGCTGATGATCTTG-3’
ATM F	5’-CTTGTGCCTTGGCTACAGAT-3’
ATM R	5’-AGACAGCTCACAGTTAGGTAAAC-3’
p53 F	5’-GAGCTGAATGAGGCCTTGGA-3’
p53 R	5’-CTGAGTCAGGCCCTTCTGTCTT-3’
CRISPR screening*	
mH2A1.2 KO F	5’-GCTTTGAGGTGGAGGCCATAATCA-3’
mH2A1.2 KO R	5’- GGAAGAGAATTCAGATGGCAATG -3’

Table S3, related to STARS Methods. Primer sequences. Annealing temperatures were 58 °C,* denotes touchdown PCR.

Sample_ID	Cell type	Treatment	CHIP	Total reads	Mapped	Percent map
N_2_mH2A1	K562 WT	Untreated	mH2A1	193,974,054	187,203,324	96.51%
N_2_mH2A1_Inp	K562 WT	Untreated	Input	167,746,400	162,047,094	96.60%
N_1_mH2A1	K562 WT	Untreated	mH2A1	193,989,626	187,109,720	96.45%
N_1_mH2A1_Inp	K562 WT	Untreated	Input	170,879,968	164,814,920	96.45%
Aph_0.5_2_mH2A1	K562 WT	Aphidicolin	mH2A1	168,053,504	124,124,565	73.86%
Aph_0.5_2_mH2A1_Inp	K562 WT	Aphidicolin	Input	222,705,751	167,659,900	75.28%
Aph_0.5_1_mH2A1	K562 WT	Aphidicolin	mH2A1	158,722,533	116,816,127	73.60%
Aph_0.5_1_mH2A1_Inp	K562 WT	Aphidicolin	Input	214,827,126	161,288,068	75.08%
K562_A1_12	K562 WT	Aphidicolin	mH2A1.2	40,951,559	39,935,534	97.52%
K562_A1_Inp	K562 WT	Aphidicolin	Input	45,997,458	44,522,652	96.79%
K562_A3_12	K562 WT	Aphidicolin	mH2A1.2	37,165,463	36,350,530	97.81%
K562_A3_Inp	K562 WT	Aphidicolin	Input	48,422,653	47,162,513	97.40%
K562_N3_12	K562 WT	Untreated	mH2A1.2	41,985,369	40,941,207	97.51%
K562_N3_Inp	K562 WT	Untreated	Input	40,928,973	39,789,229	97.22%
K562_N1_12	K562 WT	Untreated	mH2A1.2	44,176,387	43,122,374	97.61%
K562_N1_Inp	K562 WT	Untreated	Input	41,921,556	40,816,944	97.37%
Aph_0.5_2_rH2Ax	K562 WT	Aphidicolin	gH2Ax	205,990,428	153,695,346	74.61%
Aph_0.5_1_rH2Ax	K562 WT	Aphidicolin	gH2Ax	196,515,410	145,895,753	74.24%
K562_A1_gH2Ax	K562 WT	Aphidicolin	gH2Ax	56,900,760	55,425,455	97.41%
K562_A3_gH2Ax	K562 WT	Aphidicolin	gH2Ax	48,492,804	47,233,781	97.40%
K562_N3_gH2Ax	K562 WT	Untreated	gH2Ax	52,524,001	50,854,726	96.82%
K562_N1_gH2Ax	K562 WT	Untreated	gH2Ax	53,162,702	51,538,217	96.94%
N_1_rH2Ax	K562 WT	Untreated	gH2Ax	183,516,394	176,881,163	96.38%
N_2_rH2Ax	K562 WT	Untreated	gH2Ax	173,604,198	167,281,913	96.36%
2A3-Aph-Inp-1	1.2 KO	Aphidicolin	Input	52,219,220	51,016,012	97.70%
2A3-Aph-gH2Ax-1	1.2 KO	Aphidicolin	gH2Ax	54,164,970	52,570,385	97.06%
2A3-N-Inp-1	1.2 KO	Untreated	Input	63,148,550	61,730,491	97.75%
2A3-N-gH2Ax-1	1.2 KO	Untreated	gH2Ax	50,216,044	48,676,674	96.93%
K562-Aph-Inp-1	K562 WT	Aphidicolin	Input	51,096,493	50,024,120	97.90%
K562-Aph-gH2Ax-1	K562 WT	Aphidicolin	gH2Ax	45,358,908	44,107,351	97.24%
K562-N-Inp-1	K562 WT	Untreated	Input	59,167,024	57,874,301	97.82%
K562-N-gH2Ax-1	K562 WT	Untreated	gH2Ax	48,778,895	47,511,179	97.40%
K562-F10-N2-Inp	K562 sh-RFP	Untreated	Input	39,045,539	38,017,676	97.37%
K562-F10-N2-1-2	K562 sh-RFP	Untreated	mH2A1.2	39,325,104	38,316,666	97.44%
K562-C11-N2-Inp	K562 sh-mH1.2	Untreated	Input	46,273,053	45,023,681	97.30%
K562-C11-N2-1-2	K562 sh-mH1.2	Untreated	mH2A1.2	39,967,414	38,835,535	97.17%

Table S4, related to Figures 1, 4, S1 and S4. Summary of sequencing experiments

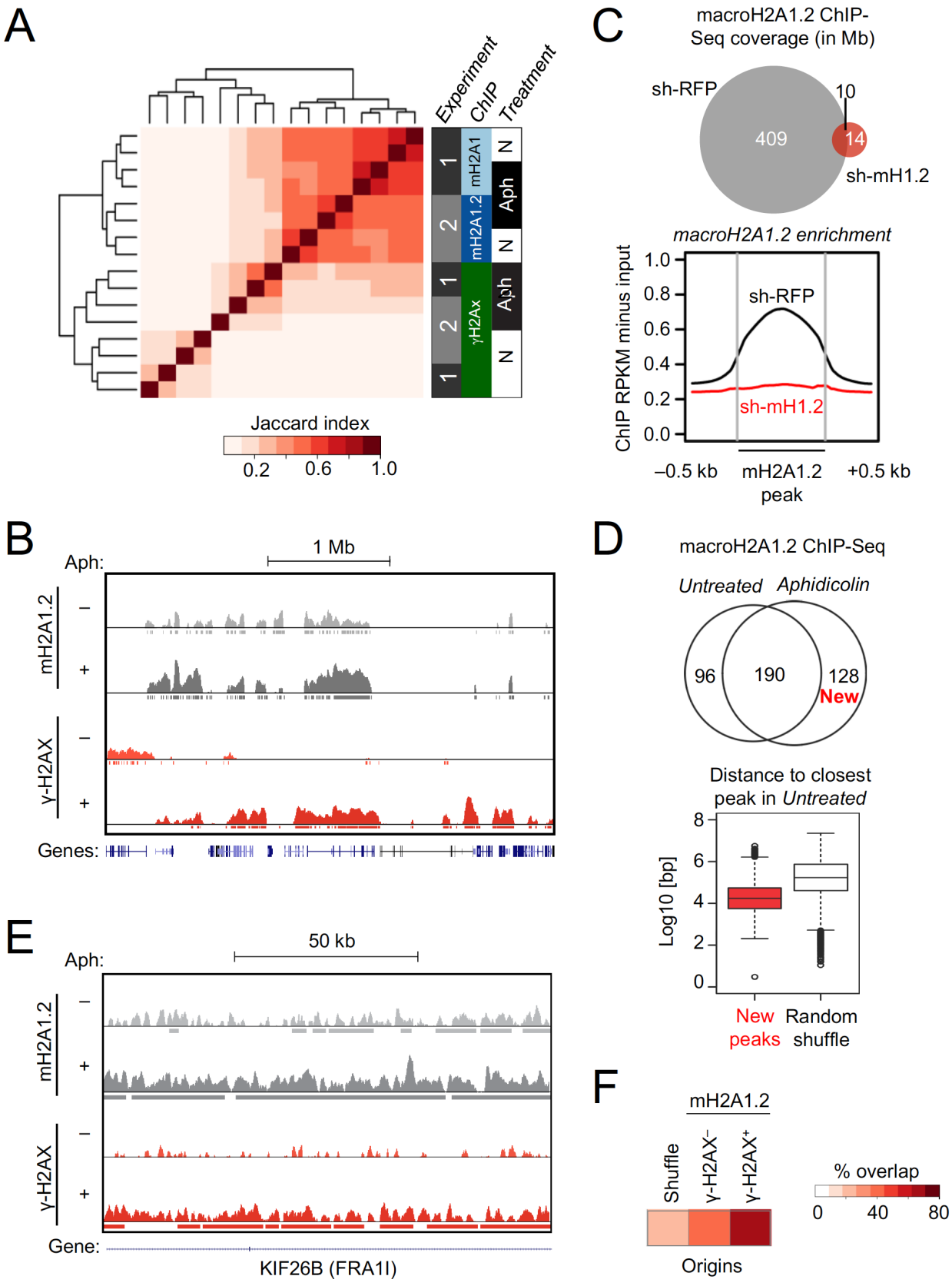
A
Experiment
ChIP
Treatment
1
2
mH2A1
mH2A1.2
γH2Ax
N
Aph
Jaccard index
0.2
0.6
1.0
B
Aph:
1 Mb
mH2A1.2
γ-H2AX
Genes:
C
macroH2A1.2 ChIP-Seq coverage (in Mb)
sh-RFP
10
409
14
sh-mH1.2
macroH2A1.2 enrichment
ChIP RPKM minus input
1.0
0.8
0.6
0.4
0.2
0.0
sh-RFP
sh-mH1.2
–0.5 kb
mH2A1.2 peak
+0.5 kb
D
macroH2A1.2 ChIP-Seq
Untreated
Aphidicolin
96
190
128
New
Distance to closest peak in Untreated
Log10 [bp]
8
6
4
2
0
New peaks
Random shuffle
E
Aph:
50 kb
mH2A1.2
γ-H2AX
Gene:
KIF26B (FRA1I)
F
mH2A1.2
Shuffle
γ-H2AX⁻
γ-H2AX⁺
Origins
% overlap
0
40
80

Figure S1, related to Figure 1. Characterization of RS-induced macroH2A1.2 accumulation genome-wide. (A) Jaccard index (intersection in base pairs divided by the sum of the union and intersection) for ChIP-Seq peaks. Experiment, ChIP target, and treatment are indicated with a color-coded bar. Results are presented in a heatmap with hierarchical clustering. N: untreated, Aph: Aphidicolin, all experiments were performed in K562 cells. (B) Browser view of macroH2A1.2 and γ-H2AX ChIP enrichment within FRA1I region. Data are log2 ChIP/Input. Each track is displayed on the same scale (ranging from 0 to 2). (C) Venn diagram of overlap of macroH2A1.2 ChIP-Seq peaks called in control (sh-RFP) and macroH2A1.2 knockdown (sh-mH1.2). Line plot below shows macroH2A1.2 enrichment for the indicated samples within macroH2A1.2 peaks identified based on sh-RFP ChIP-Seq. (D) Venn diagram highlighting new macroH2A1.2 peak coverage induced upon Aph treatment. Box plot below shows the proximity of Aph-induced macroH2A1.2 peaks (new peaks) to macroH2A1.2 peaks in untreated samples compared to a random shuffle control. (E) Browser view of macroH2A1.2 and γ-H2AX ChIP enrichment within a zoomed section of the region depicted in Fig. 1D. Data are log2 ChIP/Input. Each track is displayed on the same scale (ranging from 0 to 2). Horizontal bars indicate peak coverage. (F) Overlap of macroH2A1.2 peaks with replication origins, shown as a heatmap, with shuffled control for comparison. MacroH2A1.2 peaks are subdivided based on overlap with γ-H2AX (γ-H2AX^{+} and γ-H2AX^{-}).

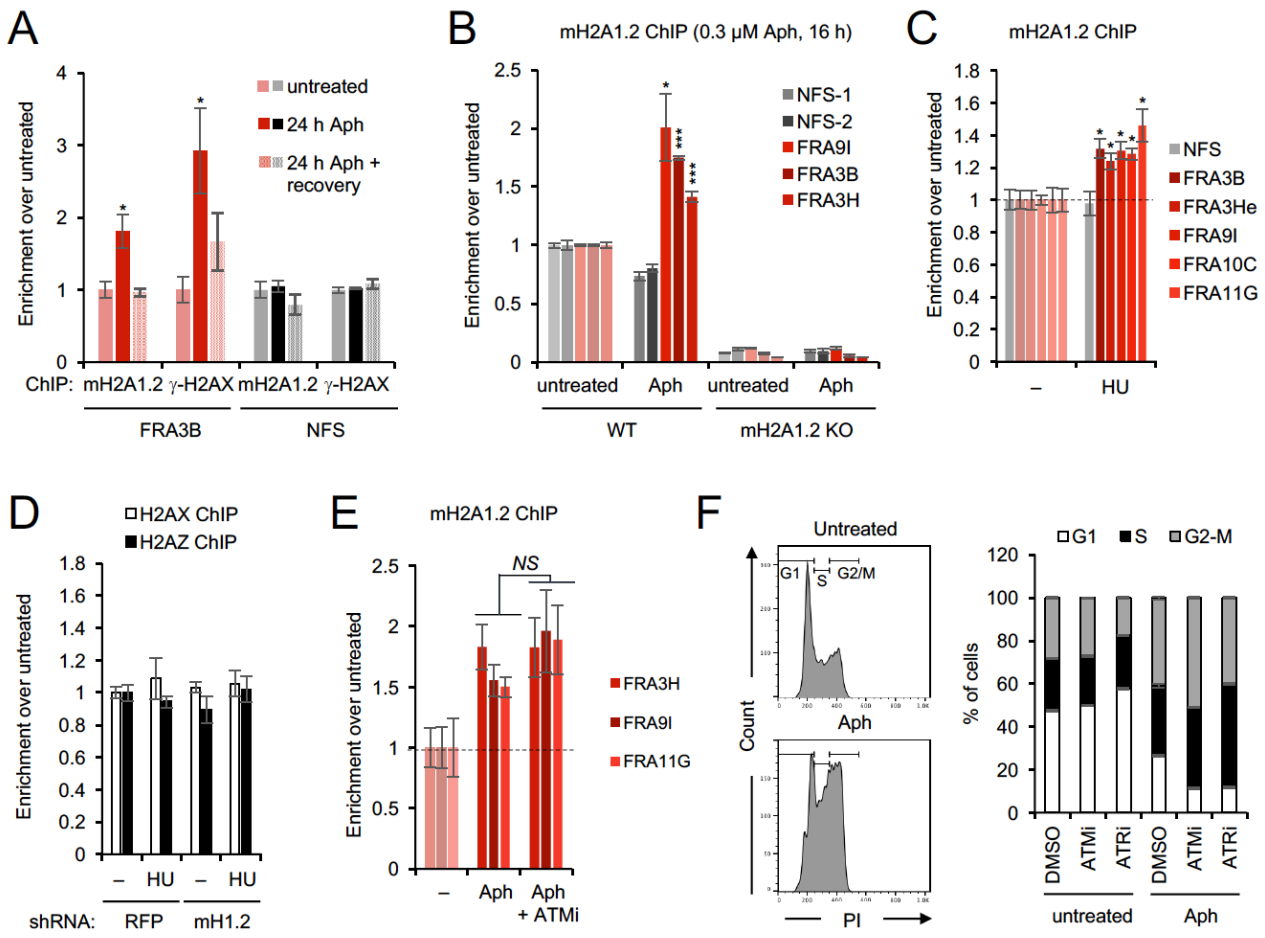

Figure S2, related to Figure 1, 6. RS-induced macroH2A1.2 accumulation at CFSs and its DDR dependence. (A) ChIP analysis for γ-H2AX or macroH2A1.2 in K562 cells treated with Aph for 24 h with or without 24 h recovery. Enrichment relative to untreated samples is shown at the indicated loci. Values represent mean and SEM (n = 3). (B) ChIP for macroH2A1.2 in macroH2A1.2 CRISPR knockout cells (KO) or parental K562 controls (WT) in the presence or absence of 16 h treatment with 0.3 μM Aph. Enrichment relative to untreated samples is shown at the indicated CFSs. (C) ChIP for macroH2A1.2 in K562 cells in the presence or absence of hydroxyurea (HU) treatment, analyzed as in (A). (D) ChIP for H2AX or H2AZ in cells expressing the indicated shRNAs. Enrichment at FRA9I is shown relative to untreated sh-RFP samples. (E) ChIP for macroH2A1.2 as in (B), in the presence or absence of Aph and ATM inhibitor. Enrichment relative to untreated samples is shown at the indicated CFSs. (F) Cell cycle analysis in K562 cells that were either treated with Aph or left untreated in the presence or absence of ATM or ATR inhibitor (ATMi, ATRi). Propidium Iodide (PI) staining was used to determine DNA content. Samples were analyzed in triplicate, values are expressed as mean and SD. A representative histogram is shown. Values in (A-D) are expressed as mean and SEM (n = 3). Unless noted otherwise, p values are based on Student's two-tailed *t-test* and expressed relative to the RS-exposed NFSs, * $p < 0.05$, ** $p < 0.01$ and *** $p < 0.001$.

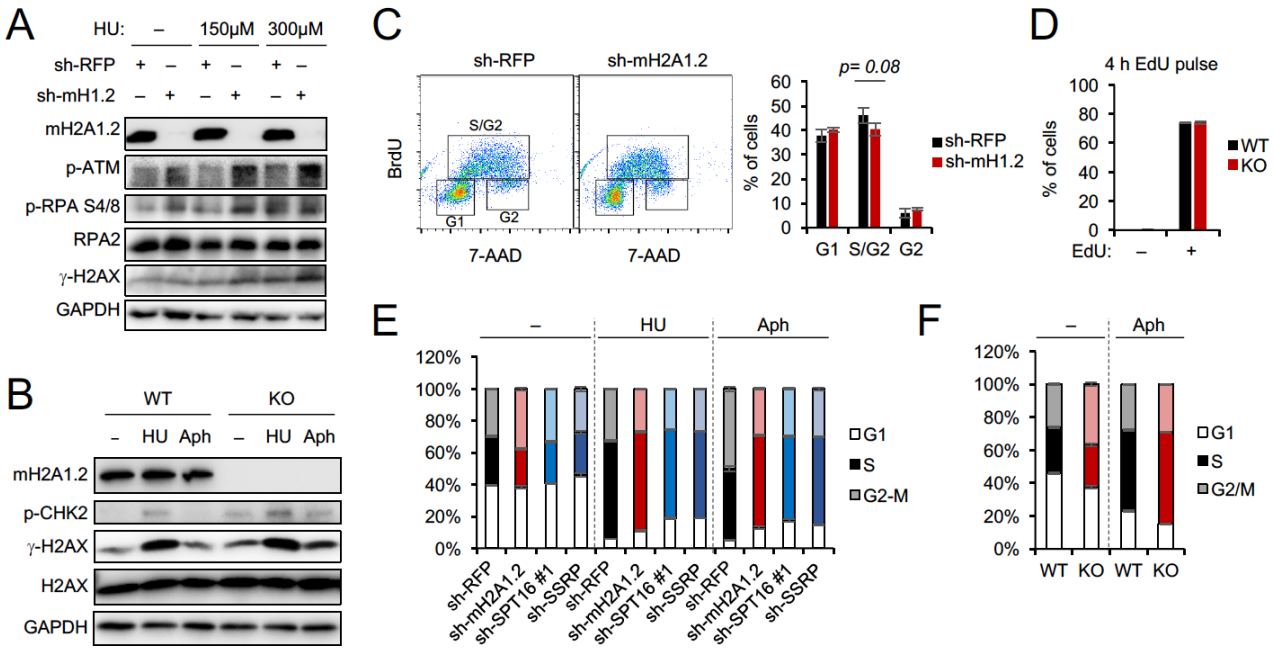

Figure S3, related to Figures 3, 4. Impact of macroH2A1.2 depletion on DDR signaling and cell cycle. (A) Western blot analysis for markers of DSB repair in the presence or absence of HU in macroH2A1.2 depleted cells (sh-mH1.2) or sh-RFP-expressing controls. (B) Western blot analysis for markers of DSB repair in the presence or absence of HU or Aph in WT or macroH2A1.2 KO K562 cells. Note that DNA damage induction upon exposure to low dose HU (300 μM) was overall more pronounced than upon exposure to low dose Aph (0.5 μM). (C) Cell cycle distribution following shRNA-mediated depletion of macroH2A1.2. 5-Bromo-2'-deoxyuridine (BrdU) and 7-AAD staining shows S phase cells and DNA content, respectively. Samples were analyzed by FACS in triplicate. A representative dot plot is shown. Values for the indicated gates are expressed as mean and SD. (D) Frequency of S-phase cells in macroH2A1.2 KO cells and WT controls based on 5-ethynyl-2'-deoxyuridine (EdU) incorporation. Cells were analyzed by FACS. Values are expressed as mean and SD (n=2). (E) PI analysis of cell cycle distribution in cells expressing the indicated shRNAs in the presence or absence of replication stress (HU or Aph). Samples were analyzed by FACS in triplicate, cell cycle stages are as in Fig. S2E. Values are expressed as mean and SD. (F) Cell cycle distribution in macroH2A1.2 WT or KO cells in the presence or absence of Aph. PI staining was used to determine DNA content. Samples were analyzed in duplicate as in (E).

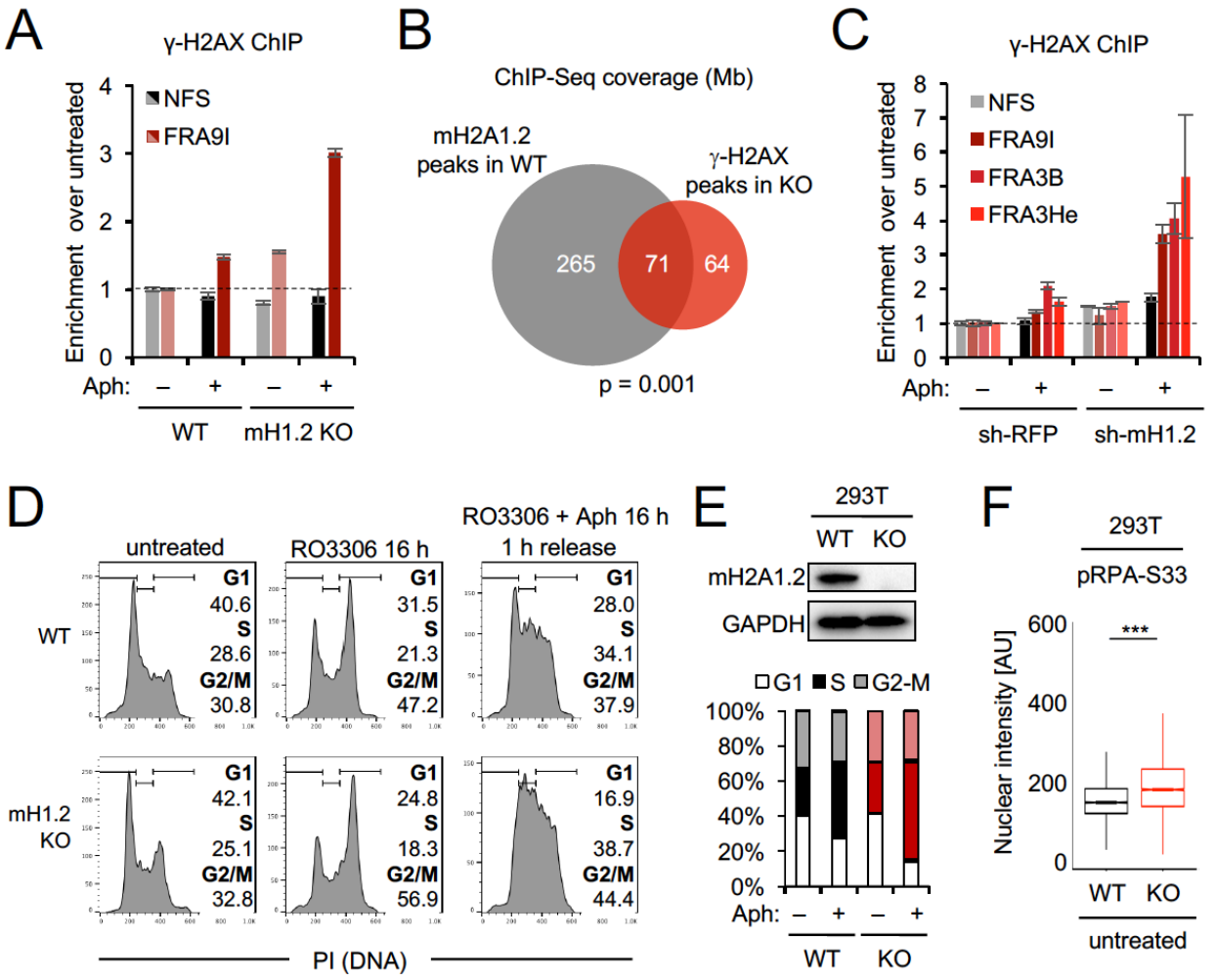

Figure S4, related to Figure 4. Impact of macroH2A1.2 depletion on RS-induced DNA damage. (A) ChIP analysis for γ-H2AX in macroH2A1.2 WT or KO cells in the presence (dark bars) or absence of Aph (light bars). Enrichment relative to untreated WT is shown at FRA9I or a non-fragile site (NFS). Values are expressed as mean and SEM (n = 3). (B) Overlap in base pairs between macroH2A1.2 peaks in WT K562 cells with γ-H2AX peaks in macroH2A1.2 KO cells in the presence of Aph. The indicated p-value is the result of a permutation test (N = 1,000 trials). (C) ChIP analysis for γ-H2AX in K562 cells expressing the indicated shRNA in the presence (dark bars) or absence of Aph (light bars). Enrichment relative to untreated sh-RFP controls is shown at the indicated loci. Values are expressed as mean and SD from two (FRA9I, FRA3He) or three independent experiments (FRA3B). (D) PI analysis of cell cycle distribution in macroH2A1.2 WT or KO cells treated with the indicated drugs. G1, S and G2 content is indicated. Samples were analyzed by FACS in triplicate, one of three representative experiments is shown. (E) Western blot and PI cell cycle analysis of macroH2A1.2 CRISPR/Cas9 KO (KO) 293T cells or parental WT cells. Values for PI analysis are expressed as mean and SD (n = 2). (F) IF analysis of pRPA-S33 in 293T cells. Box plots depict total pRPA-S33 nuclear intensities in WT (n = 4717 cells) or KO cells (n = 3849 cells). Cells were combined from three independent experiments, *** denotes $p < 0.001$ by Mann-Whitney U test.

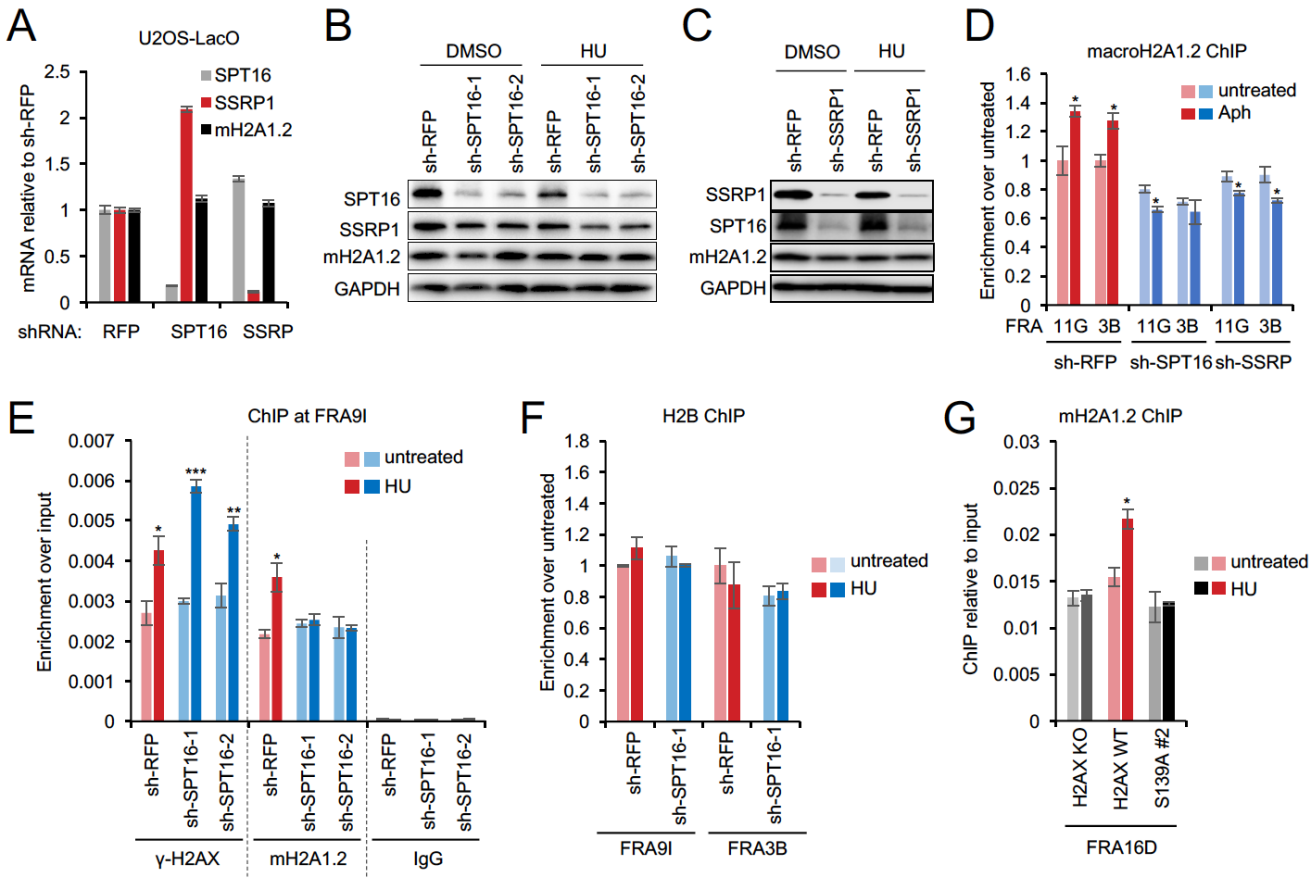

Figure S5, related to Figure 5. Impact of FACT and H2AX on RS-induced macroH2A1.2 accumulation at CFSs. (A) RT-PCR analysis of indicated mRNA expression levels relative to GAPDH in U2OS cells expressing the indicated shRNAs. Values were normalized to sh-RFP and are expressed as mean and SD (n = 3). (B, C) Western blot analysis for SUPT16H (SPT16), SSRP1, or macroH2A1.2 in K562 cells expressing the indicated shRNAs in the presence or absence of HU treatment. (D) ChIP analysis for macroH2A1.2 in K562 cells expressing the indicated shRNA in the presence or absence of 0.3 μM Aph (16 h). Enrichment relative to the untreated sh-RFP sample is shown for the indicated CFSs. (E) ChIP analysis for γ-H2AX, macroH2A1.2, or IgG in K562 cells expressing the indicated shRNA in the presence or absence of HU. Enrichment relative to input is shown for the FRA9I CFS. (F) ChIP analysis for H2B at the indicated CFSs in the presence or absence of HU. Enrichment relative to untreated sh-RFP cells is shown. (G) ChIP analysis for macroH2A1.2 in the presence or absence of HU in H2AX KO HCT116 cells (H2AX KO) and H2AX KO cells reconstituted with WT (H2AX WT) or S139A mutant H2AX (S139A #2). S139A #2 is a second, independent S139A clone distinct from Fig. 4C. Enrichment relative to input is shown. Unless noted otherwise, all values are expressed as mean and SEM (n = 3).

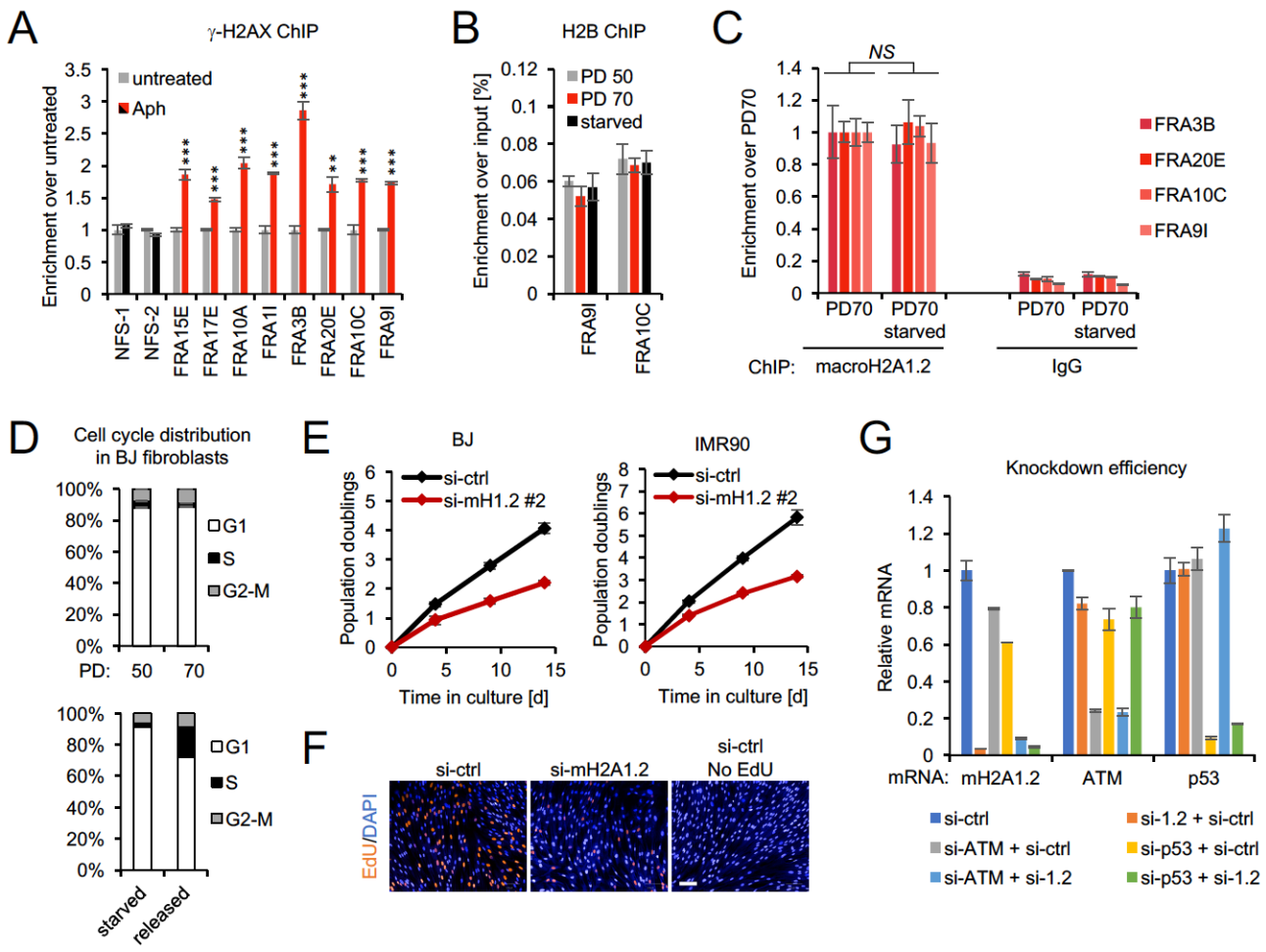

Figure S6, related to Figure 6. macroH2A1.2 function in primary fibroblasts. (A) ChIP analysis for γ-H2AX in untreated or Aph-treated BJ fibroblasts. Enrichment relative to untreated samples is shown for the indicated CFSs and NFS control loci. (B) ChIP analysis for H2B in population doubling (PD) 50, PD 70, or starved BJ fibroblasts. Enrichment relative to input is shown at the indicated CFSs. (C) ChIP analysis for macroH2A1.2 and IgG in PD 70 BJ fibroblasts that were either left untreated or serum-starved for 72 h. Enrichment relative to input is shown for the indicated CFSs. Unless noted otherwise, values represent mean and SEM (n=3). (D) PI-based cell cycle profiling in PD 50 or PD 70 BJ fibroblasts as well as BJ cells serum-starved for 72 h. A 22 h release from serum starvation is shown as a control. Values for the indicated cell subsets represent mean and SD (n = 3). (E) Analysis of PDs in BJ and IMR90 fibroblasts after macroH2A1.2 knockdown using a second, independent siRNA against macroH2A1.2 (si-mH1.2 #2). Values are expressed as mean and SD (n = 3). (F) EdU labeling of S phase IMR90 fibroblasts in the presence of the indicated siRNAs. EdU incorporation was analyzed by IF, nuclei were counterstained with DAPI. Representative images are shown, no EdU served as a negative control. The fraction of EdU^+ cells was determined in triplicate for analyses in Fig. 5E. Scale bar, 100 µm. (G) RT-PCR analysis of knockdown efficiencies in IMR90 cells analyzed in Fig. 5E. RNA was normalized to rpl13a and β-actin, values are relative to si-control and expressed as mean and SD (n = 2).